Optimum Detection of Frequency-Hopped Signals'

Unjeng Cheng
Barry K. Levitt
Andreas Polydoros
Marvin K. Simon

Jet Propulsion Laboratory
California Institute of Technology
4800 Oak Grove Drive
Pasadena, California 91109

November 10, 1992

Abstract

This paper derives and analyzes optimum and near-optimum structures for detecting frequency-hopped (FH) signals with arbitrary modulation in additive white Gaussian noise. The principal modulation formats considered are M-ary frequency-shift-keying (MFSK) with fast frequency hopping (FFH) wherein a single tone is transmitted per hop, and slow frequency hopping (SFH) with multiple MFSK tones (data symbols) per hop. The SFH detection category has not previously been addressed in the open literature and its analysis is generally more complex than FFH. A special subset of the SFH/MFSK format that receives particular attention in this paper is the case of continuous-phase modulation (CPM) for which the carrier phase is assumed to be constant over the entire hop.

The major contributions of this article are twofold. (1) It presents a detailed discussion of the modeling assumptions involved in deriving optimum FH detectors in the classical, average-likelihood ratio detection theory sense, relating them to previously published results and clarifying some persistent misconceptions about claims of optimality. (2) It attempts the most thorough performance evaluation of these structures to date by employing recently developed novel techniques for accurate computer simulation of the true system performance.

A fundamental conclusion is that SFH/CPM modulation is advantageous not only to the communicator but also to a sophisticated noncoherent detector. By applying techniques developed in this paper to exploit the continuous-phase characteristic, a detector of reasonable complexity will perform appreciably better than traditional channelized detectors such as the filter-bank combiner.

'This work was performed by the Jet Propulsion Laboratory, California Institute of Technology, under a contract with the National Aeronautics and Space Administration.

1. Introduction

Within both the civilian commercial and tactical military arenas, there is a rapidly growing trend toward the use of spread-spectrum (SS) communication systems in general and frequency-hopped (FH) systems in particular because of their inherent anti-jam or anti-interference and low-probability-of-intercept characteristics. There has been a concomitant interest from both sectors in the ability of unauthorized receivers to detect FH emissions. Many *ad hoc* FH detection structures have been proposed which typically incorporate a fast-Fourier-transform (FFT) or other channelized front-end preprocessor. The performances of some of these signal processors have been tested in the field, simulated in computers or occasionally analyzed, sometimes giving rise to questionable superiority claims. However, these exercises generally neglect the issue of fundamental performance limits unrestricted by practical implementation constraints and the notion of optimality in the classical average-likelihood ratio (ALR) detection theory sense [1], which is the subject of this paper.

The problem of detecting an FH signal imbedded in additive white Gaussian noise (AWGN) based on the observation of a *single* received hop (dwell) is similar to the standard radar problem of detecting a Doppler-shifted target return assuming that the unknown frequency shift is discretized to a finite number of possible values [2], [3]. In this analogy, the number N_c of possible FH frequency channels (hop frequencies) corresponds to the number of Doppler frequency resolution cells, and both detectors could employ a channelized FFT front end with appropriate post-FIT processing.

However, there are some fundamental differences between the two problems that lead to divergent solutions. In particular, FH detectors typically observe many consecutive hops wherein the carrier jumps pseudorandomly from one frequency channel to another, and the detector is assumed to have no *a priori* information about this hopping pattern. Furthermore, unlike the radar case, FH signals are often 10s or 100s of MHz wide, with NC on the order of 1000 or more. Another significant difference is that the FH carrier usually has data modulation, which may be of value to a properly designed detector. In summary, the FH detection problem is simultaneously more complicated than its radar counterpart, yet more susceptible to exploitation by sophisticated signal processing techniques.

Many results have been published in the area of noncoherent (i.e., unknown carrier phase) envelope detection of “narrowband” (fixed, known frequency) [3] - [5] and "wideband" (unknown frequency) radar returns [2], [6], [7]. For a unity time-bandwidth product (TBP), envelope detection is equivalent to radiometric (energy) detection. This has prompted analysts to treat the latter as a common yardstick of minimum performance even for large TBPs [8] for which radiometric detection has no other claims of suitability other than simplicity and robustness to signal feature variations. (In fact, in the absence of any knowledge about the received signal characteristics other than its frequency band, the radiometer may be the only pragmatic detector available.) The general conclusions that have emerged from this significant body of work are as follows. (1) Radiometric detection can be quite inferior to channelized structures for large values of N_c (i.e., when the temporary spectral occupancy of the signal is small compared to the total observed bandwidth). (2) Adaptive spectral estimation techniques can produce major performance improvements relative to fixed FFT preprocessors when there is a mismatch between the actual and measured frequency channels. (3) For small values of NC and variable signal amplitude (fading) there is only a minor performance gap between the optimum ALR and maximum-

likelihood ratio (MLR) schemes, wherein we jointly detect the presence of the received signal and estimate one or more signal features (e.g., the FH pattern or the imbedded data).

Early papers on FH signal processing concentrated on the exploitation of cyclic features derived from nonlinear operations on the received signal (e.g., delay-and-multiply structures fordetermining hoptiming epoch information [9]); such procedures are useful, but are *ad hoc* in nature and generally far from optimum. A more fundamental ALR analysis resulted in an influential series of reports which derived the first optimum detectors for multiple-hop observations of FH signals with unknown data modulation [10] - [12]. Woodring and Eden approximated the performance of these detectors based on inaccurate central-limit theorem (CLT) arguments. The analysis of various multiple-hop decision combining methods was detailed in [13] and [14]. Subsequent publications described and compared these detectors in depth, assessing their practical limitatations [15, Vol. Ill], [16], [17], analyzing their performance in more theoretical detail and with greater accuracy [18], and proposing alternative implementation techniques for improved performance [19] - [23].

All of these earlier papers were restricted to or optimized for fast frequency-hopped (FFH) waveforms with *M*-ary frequency-shift-keyed (MFSK) data modulation wherein a single MFSK symbol is transmitted in each hop. For this class of signals, the transmitted waveform consists of a single tone of constant amplitude in each hop, so that the optimum noncoherent receiver per hop (assuming a distortion-free channel) is simply an envelope detector with unity TBP followed by a Bessel function operation because of the uniformly distributed unknown carrier phase. Although other FH waveforms have been discussed before with higher TBPs, most notably, the hybrid direct-sequence (DS)/FH case in [11] and [12], the resulting detectors are only optimum conditioned on a specific front-end preprocessor as discussed in more detail below for the Woodring-Edell (WE) implementation. One of the contributions of this paper is to identify and clarify such misconceptions.

This paper begins with a review of some previously published wideband and FH detectors from a classical detection theoretic perspective. Coherent and noncoherent optimum ALR detectors are then derived for FFH/MFSK signals and slow frequency-hopped (SFH)/MFSK signals in which the carrier phase is discontinuous from symbol to symbol. The more difficult analytical problem of SFH signals with arbitrary continuous-phase modulation (CPM) is then considered and specialized to the case of continuous-phase MFSK (CPFSK). The optimum general SFH/CPM detector is found to have an impractical complexity that grows exponentially with the number of symbols per hop; for the special case of SFH/CPFSK signals with integer sub-multiple modulation indices, an alternative implementation with linear complexity growth and negligible loss of optimality is derived. Some nearly optimum MLR simplifications are explored in which the signal is detected and features such as the imbedded data or the FH pattern are simultaneously estimated. Novel statistical models described in two companion papers [24], [25] are used to accurately compare the performance of these SFH detectors with the traditional wideband radiometer, the WE detector and the filter-bank combiner (FBC). In this last case, threshold tests are performed within each FH channel on each observed hop [15, Vol. Ill, pp. 295-305].

II. Review of Some Previously Published Suboptimum FH Detectors

A. Arbitrary Wideband Signals: Radiometer

The most general formulation of the classical signal detection problem seeks to determine whether a bandlimited signal s(t) has been received in additive white Gaussian noise (AWGN) $n(t)$ based on the observation of the composite received signal $r(t)$ over the observation interval (O, T):

$$r(t) = \begin{cases} s(t) + n(t); & H_1 \\ n(t); & Ho \end{cases} \tag{1}$$

where H_1 and H_0 are respectively the signal present and signal absent hypotheses. It is assumed that $s(t)$ has RF bandwidth W and $n(t)$ has two-sided power spectral density $N_0/2$. In the absence of any further *a priori* information about the specific characteristics of s(t) such as its modulation, the simple radiometer of Fig. 1 is often used to distinguish between the two hypotheses [15, Vol. III, pp. 288-290]," [26, pp. 128-135]. This detector does not use received carrier phase information so it falls into the noncoherent category.

For large TBPs, $TW > 1$, the sampling theorem can be used to show that the radiometer output R is essentially a noncentral (H_1) or central (H_0) chi-square (χ^2) random variable (RV) with $2TW$ degrees of freedom [16, (4.28), (4.30)]:

$$p(R) = \begin{cases} \frac{1}{N_0}\left(\frac{R}{E}\right)^{\frac{TW-1}{2}} e^{-\frac{R+E}{N_0}} I_{TW-1}\left(\frac{2}{N_0}\sqrt{ER}\right); & H_1,\ R \geq 0 \\ \frac{1}{2\,\Gamma(TW)}\left(\frac{R}{N_0}\right)^{TW-1} e^{-\frac{R}{N_0}}; & H_0,\ R \geq 0 \\ 0; & R < 0 \end{cases} \tag{2}$$

where E is the total energy in $s(t)$ over T. It is commonly believed that this result is approximately valid for smaller TBPs, including the limiting case $TW = 1$, although this has not been demonstrated analytically with any rigor. The threshold η in Fig, 1 is used to trade off the probability of a false alarm, P_{FA}, and the probability of a miss, P_M, which traditionally define detector performance:

$$P_{FA} \equiv \int_{\eta}^{\infty} dR\ p(R|H_0) \qquad PM \equiv \int_{0}^{\eta} dR\ p(R|H_1) \tag{3}$$

For $TW > 1$, CLT arguments are usually invoked to approximate the χ^2 RV R in (2) by a Gaussian RV (GRV) under H_1 or H_0; then (3) yields the familiar performance equation [15, Vol. III, (4.4) and (4.5)]:

$$\gamma \equiv \frac{S}{N_0 W} \approx \frac{1}{\sqrt{TW}} \left[Q^{-1}(P_{FA}) - \sqrt{1+2\gamma}\, Q^{-1}(1-PM)\right];\ TW > 1$$

$$\approx \frac{1}{\sqrt{TW}} \left[Q^{-1}(P_{FA}) - Q^{-1}(1-P_M)\right];\ \gamma < \frac{1}{2} \qquad (4)$$

where γ is the ratio of the received signal power $S = E/T$ to the noise power $N_0 W$ and Q^{-1} is the inverse of the Gaussian probability integral. Although the wideband radiometer performs much worse than more sophisticated detectors if additional information about the characteristics of the received signal is available (e.g., the modulation format), its appeal lies in its minimal complexity and robustness (i.e., its insensitivity to variations in the signal features). In particular, if s(t) is an FH signal, the radiometer does not require frequency channel and hop timing epoch synchronization.

B. FH **Signals** with Arbitrary Modulation: **Channelized** Detector

Now suppose s(t) is an FH signal with total SS bandwidth W_{ss}, hop rate R_h, hop dwell time $T_h = 1/R_h$, and received signal energy per hop $E_h = ST_h$. The baseband data modulation at this point is arbitrary, but the combination of this modulation with the FH carrier naturally partitions W_{ss} into NC contiguous, non-overlapping channels, each with bandwidth $W_m = W_{ss}/N_c$, such that the entire signal energy in any hop lies within a single channel. As discussed below, these NC FH channels do not always correspond to the unmodulated FH carrier frequencies. Nonetheless, for reasons of mutual orthogonality between the channels, the TBP $T_h W_m$ is a positive integer, Also, for analytical simplicity, assume that the detector observation interval (O, T) contains an integer number $N_h = T/T_h$ of complete hops.

If the radiometer above were used to detect this FH signal, Fig. 1 and *(2)-(4)* are still applicable with the obvious substitution $W = W_{ss}$. However, the detector performance can be further improved by exploiting its limited knowledge of the FH signal features. In the usual idealized signal detection formulation, the detector is assumed to have somehow achieved frequency and time synchronization with the received signal, i.e., it knows R_h, the location of the FH channels in the frequency domain, and hop timing (in practice, it would have to extract these characteristics from the received signal). Because of the channelized nature of the FH signal and the arbitrary data modulation, it is not unreasonable for an *ad hoc* detector to prefilter the received signal with a matching bank of NC contiguous, non-overlapping bandpass energy detectors of the form in Fig. 1, each with bandwidth W_m and integration time T_h aligned with the received hops: this preprocessor is typically called a *channelized radiometer* [26, pp. 135-140].

Denote the outputs of this preprocessor for the ith hop by the random vector, $R_i = \{R_{ij};\ j = 1, 2, \ldots, N_c\}$ where the RV R_{ij} corresponds to the jth FH channel. As in (2), each R_{ij} is approximately χ^2 with $2T_h W_m$ degrees of freedom. Under H_1, the component corresponding to the FH channel that contains the signal on the ith hop is noncentral χ^2 and the remaining NC- 1 are central χ^2; under H_0, all of them are central χ^2. The complete observable over (O, T) is $R = \{R_i;\ i = 1, 2, \ldots, N_h\}$, and all $N_h N_c$ components are statistically independent (S1). From (2),

$$\frac{p(R_i|H_1,\omega_j)}{p(R_i|H_0)} = \frac{p(R_{ij}|H_1,\omega_j)}{p(R_{ij}|H_0)}$$

$$= 2\,\Gamma(T_hW_m)\,N_0^{T_hW_m-2}\,(E_hR_{ij})^{\frac{T_hW_m-1}{2}}\,e^{-\frac{E_h}{N_0}}\,I_{T_hW_m-1}\left(\frac{2}{N_0}\sqrt{E_hR_{ij}}\right) \tag{5}$$

Since the signal is equally likely to lie in any of the NC channels on a given hop, the ALR based on $\boldsymbol{R}$ reduces to

$$\Lambda(\boldsymbol{R}) \equiv \frac{p(\boldsymbol{R}|H_1)}{p(\boldsymbol{R}|H_0)} = \prod_{i=1}^{N_h}\frac{1}{N_c}\sum_{j=1}^{N_c}\frac{p(R_i|H_1,\omega_j)}{p(R_i|H_0)}$$

$$\propto \prod_{i=1}^{N_h}\sum_{j=1}^{N_c} R_{ij}^{\frac{T_hW_m-1}{2}}\,I_{T_hW_m-1}\left(\frac{2}{N_0}\sqrt{E_hR_{ij}}\right) \tag{6}$$

The last line of (6) is a sufficient statistic for the ALR, as first proposed by Woodring and Eden [11]. Since $\boldsymbol{R}$ is not generally a sufficient observable for the original received signal *r(t),* and because its components are only approximately χ^2, the WE FH detector cannot truly be optimum in the classical ALR sense. Nonetheless, in the absence of information about the specific data modulation, and *conditioned on a channelized radiometer preprocessor, (6)* is the optimum noncoherent ALR detection metric for FH signals. Unfortunately, the perception that the WE structure is the *unconditionally* optimum FH detector has been perpetuated in the literature (e.g., [15, Vol. III, pp. 290-295], [27, p. 15]), usually for the special case $T_hW_m = 1$ where the χ^2 approximation is weakest but (6) simplifies to the sufficient statistic

$$A(R) \propto \prod_{i=1}^{N_h}\sum_{j=1}^{N_c} I_1\left(\frac{2}{N_0}\sqrt{E_hR_{ij}}\right);\ T_hW_m = 1 \tag{7}$$

which is illustrated in Fig. 2.

The performance of the WE detector is approximated in [11] by a formula based on a CLT arguments. However, the Bessel operation is highly nonlinear and CLT convergence is weak for Ricean or Rayleigh arguments (i.e., the square root of the R_{ij}s, which are noncentral or central χ^2 RVS) because of the long tails in their probability density functions (PDFs), which usually leads to optimistic performance results. In computing the performance of the WE and other detectors, the results in this paper employ more accurate techniques described separately in [24] and [25].

c. Channelized Filter-Bank Combiner

A common simplification of the WE or other detectors is the FBC structure wherein a hard decision is made as to the presence of a received signal in each FH channel on each observed hop (sometimes referred to as a “frequency-time cell” in FH detector terminology)

based on a threshold comparison (e.g., [15, Vol. III, pp. 295-305]). In the WE case, because the square root, scaling and Bessel function operations in each frequency-time cell are monotonic, each channelized preprocessor output R_{ij} can equivalently be compared with a common threshold η, thereby eliminating the postprocessing complexity. As shown in Fig. 3 for the $T_h W_m = 1$ case, if this threshold is exceeded for any of the FH channels on a given hop, the presence of a signal on that hop is postulated and the OR gate generates a"1"; otherwise it outputs a "O". These intermediate hard decisions are summed over all N_h observed hops and compared with a second integer threshold L to decide on H_1 or H_0. The two thresholds are jointly optimized to minimize P_M for a desired P_{FA} and received signal-to-noise ratio (SNR). The end result is that the FBC of Fig. 3 performs much better than the wideband radiometer because it is channelized to match the FH signal, and, in fact, does almost as well the WE detector of Fig. 2 with considerably less computational complexity,

III. Derivation of Optimum FH Detectors

A. FFH/MFSK Signals

The only open literature publication of an ALR detector for FH signals without any preprocessor assumptions that we are aware of is the detector derived by Beaulieu *et al.* for FFH/MFSK signals [18].[2] For this special class, the received signal term in (1) can be represented over the ith hop by

$$s(t) = \sqrt{2S}\cos(2\pi f_j t - \theta_i);\ (l-1)T_h \le t < iT_h \tag{8}$$

where the received signal power $S = E_h/T_h$, the transmitted frequency over the ith hop is f_j corresponding to the jth FH channel, and the observation interval again contains an integer number $N_h = T/T_h$ of hops. The channel containing the signal on a given hop is equally likely to be any of the NC equally-spaced FH slots, and f_j is SI from hop to hop.[3] For the noncoherent detection case, the carrier phase over the ith hop, θ_i, is a uniformly distributed RV over (O, 2π) which is SI from hop to hop, and the minimum spacing between adjacent FH channels is $1/T_h$ for orthogonality (i.e., the modulation index $h = 1$) which implies that

[2] We use the widely accepted terminology that distinguishes between FFH and SFH signals according to whether there is a single data symbol per hop (FFH) or multiple data symbols per hop (SFH) [15, Vol. II, pp. 62-64].

[3] One of the reasons that FFH/MFSK signals are so much easier to analyze than the SFH case is that they are statistically equivalent to an unmodulated FH carrier for any alphabet size M, which suppresses the data sequence dependence.

$N_c = W_{ss}T_h$. For coherent detection,[4] the received carrier phase is assumed to be known so that $\theta_i = 0$ in (8) without loss of generality; under this condition, orthogonality occurs with a minimum FH channel separation of $1/2T_h$ (i.e., $h = \frac{1}{2}$) for which NC = $2W_{ss}T_h$.

At this point, it is appropriate to introduce the terminological distinction between the FH channels and the unmodulated carrier frequencies for *M*-ary signaling. With MFSK baseband data modulation, *M* adjacent FH channels usually form an M-ary band for a given FH carrier frequency. If these frequency bands are contiguous and non-overlapping as illustrated in Fig. 4, there are G = *NC/M* equally-spaced FH carrier frequencies or M-ary bands; in the maximally overlapping case (ignoring band edge effects), G = NC [15, Vol. II, Fig, 2.3]. This paper uses the non-overlapping format exclusively because it simplifies the SFH performance analysis. However, this restriction is only notational for now because it has no impact on either the statistical model of the received signal or the ALR detector performance in the FFH case.

It is well known that the ALR for the general signal detection problem of (1) reduces to the waveform expression [1, p. 253, (23)]

$$\Lambda[r(t)] = E_{s(t)}\left\{\exp\left[\frac{2}{N_0}\int_0^T dt\ r(t)\,s(t)\right]\right\} \qquad (9)$$

where $E_{s(t)}$ represents the expectation over the stochastic characteristics of the received signal and *E, T* and N_0 have been previously defined in conjunction with (1). For the coherent case, (9) yields the sufficient statistic [18, Fig. 1]

$$\Lambda[r(t)] \propto \prod_{l=1}^{N_h}\sum_{j=1}^{N_c}\exp\left[\frac{2}{N_0}\sqrt{E_h}\int_{(l-1)T_h}^{lT_h} dt\ r(t)\sqrt{\frac{2}{T_h}}\cos(2\pi f_j t)\right] \qquad (10)$$

In the noncoherent case, the likelihood function includes an additional expectation over the received carrier phase:

$$\Lambda[r(t)] \propto \prod_{l=1}^{N_h}\sum_{j=1}^{N_c} E_{\theta_l}\left\{\exp\left[\frac{2}{N_0}\sqrt{E_h}\int_{(l-1)T_h}^{lT_h} dt\ r(t)\sqrt{\frac{2}{T_h}}\cos(2\pi f_j t-\theta_l)\right]\right\} \qquad (11)$$

Applying the usual mathematical technique for averaging the exponential function in (11) over the random phase [1, pp. 335-348], the likelihood function reduces to the WE metric of (7):

---

[4] In practice, it is generally unrealistic for the detector to derive the received carrier phase for FFH/MFSK signals unless the hop dwell time T_h is *very* long. So the concept of coherent detection is really an idealization which serves as an upperbound performance benchmark on what is practically achievable.

$$\Lambda[r(t)] \propto \prod_{l=1}^{N_h} \sum_{j=1}^{N_c} I_0\left(\frac{2}{N_0}\sqrt{E_h R_{lj}}\right) \tag{12}$$

where

$$R_{lj} \equiv \left(\int_{(l-1)T_h}^{lT_h} dt\ r(t) \sqrt{\frac{2}{T_h}} \cos(2\pi f_j t)\right)^2 + \left(\int_{(l-1)T_h}^{lT_h} dt\ r(t) \sqrt{\frac{2}{T_h}} \sin(2\pi f_j t)\right)^2 \quad (13)$$

which is illustrated in Fig. 5 [18, Fig. 2]. However, whereas (7) was only valid for the special case of $T_h W_m = 1$, (12) holds for all TBPs. Figs. 2 and 5 also differ with regard to the preprocessor used to generate the intermediate observable $\{R_{lj}\}$. Specifically, the bank of bandpass radiometers in Fig. 2 is replaced by a bank of noncoherent inphase and quadrature (I & Q) demodulators in Fig. 5, and the order of the squaring and integration operations in each preprocessor is reversed. The net effect is that the R_{lj}s are precisely χ^2 with 2 degrees of freedom in Fig. 5 whereas they are only approximately so in Fig. 2; however, the difference between the bandpass radiometer and I & Q preprocessors is actually so small that the performance of the two detectors is almost identical over system parameter ranges of interest.

It is also interesting to compare (10) with (12)-(13) to determine the complexity impact of the coherent received carrier assumption. Although the coherent and noncoherent ALR detectors both involve the multiplication of N_h sums of N_c frequency-time cell operations, the complexity of these operations is greater for the noncoherent case. While the coherent ALR only computes the exponential function of a single quadrature demodulated component of the received signal for each frequency-time cell, the noncoherent ALR requires the formation of both the I and Q components which are then squared, summed, squarerooted and scaled before applying the zeroth-order Bessel function to the result. In fact, this observation applies to the ALR detection of SFH signals with various data modulation schemes.

Beaulieu *et al.* also introduced simplifications of their coherent and noncoherent detectors in which a threshold test is applied to each frequency-time cell, thereby eliminating the complexity of the post-R_{lj} processing [18, Figs. 3 and 4]. This variation is called MLR in [18]; however, as is evident from Fig. 6, it is really the I & Q equivalent of the bandpass-radiometer channelized FBC shown in Fig. 3.[5]

B. SFH/MFSK Signals with Discontinuous Phase

The remainder of this paper is concerned with the SFH signal detection problem, which has not been previously analyzed in the open literature. Particular attention is devoted to the combination of SFH with CPM modulation formats such as CPFSK. However, for purposes of comparison, SFH/MFSK signals in which the received carrier phase is discontinuous from symbol to symbol are considered first. Oniy the noncoherent ALR detector is derived for this

[5] In the FFH/MFSK context, a true MLR receiver might replace the average (summation) over the FH channels in the likelihood function by a maximum (i.e., select the largest), which would provide joint signal detection and FH channel estimation. However, the signal detection performance would be inferior (by definition) to the corresponding ALR receiver.

modulation format because it would be unrealistic to assume that the detector could derive the received carrier phase for each symbol. The received signal term in (1) can be represented by

$$s(t) = \sqrt{2S}\cos\left\{2\pi\left[f_j + \left(m - \frac{M-1}{2}\right)R_s\right]t - \theta_q\right\}; \quad (l-1)T_h + (l-1)T_s \le t < (l-1)T_h + lT_s \tag{14}$$

for the lth data symbol within the ith hop, where S is the received signal power, T_s is the data symbol baud time, $R_s = 1/T_s$ is the symbol rate, $E_s = ST_s$ is the received energy per symbol, and there are an integer number $N_s = T_h/T_s$ of symbols per hop. For noncoherent detection, orthogonality requires that the MFSK tones have a minimum separation of R_s (i.e., $h = 1$) which corresponds to NC = W_{ss}/R_s FH channels. With this spacing and the non-overlapping M-ary band convention of Fig. 4, f_j is the particular FH carrier frequency on the ith hop, which is equally likely to be any of $G = N_c/M = W_{ss}/MR_s$ equally-spaced frequencies that are SI from hop to hop. The fth data symbol on the ith hop is denoted by m, which is equally likely to be any integer in {O, 1, ... $M-1$} and is SI from symbol to symbol. Finally, the received carrier phase during the lth symbol in the ith hop, θ_q, is assumed to be constant, uniformly distributed over (O, 2π), and SI from symbol to symbol.

Because all of the stochastic characteristics of the received signal are at least SI from hop to hop, and the FH carrier frequencies are equally likely in a given hop, the likelihood function can be partitioned into the form

$$\Lambda[r(t)] \propto \prod_{l=1}^{N_h}\sum_{j=1}^{G}\Lambda_{ij}[r(t)\,|\,f_j] \tag{15}$$

where the condition in the argument of Λ_{ij} denotes that the FH carrier frequency over the ith hop is f_j. From (9), it follows that

$$\Lambda_{ij}[r(t)\,|\,f_j] = E_{s(t)|f_j}\left\{\exp\left[\frac{2}{N_0}\int_{(l-1)T_h}^{lT_h} dt\; r(t)s(t) - \frac{E_h}{N_0}\right]\right\} \tag{16}$$

So the likelihood function only needs to be computed for a single representative frequency-time cell in which the SS aspects of the signal are suppressed, and this partition is valid for all SFH signals of interest.

Substituting the SFH/MFSK signal of (14) into (16) and averaging over the random phase yields the representative frequency-time cell likelihood function

$$\Lambda_{ij}[r(t)\,|\,f_j] \propto \prod_{l=1}^{N_s}\sum_{m=0}^{M-1} I_0\left(\frac{2}{N_0}\sqrt{E_s R_{ijlm}}\right) \tag{17}$$

where

$$R_{ijlm} \equiv \left(\int_{(l-1)T_h+(l-1)T_s}^{(l-1)T_h+lT_s} dt\, r(t) \sqrt{\frac{2}{T_s}} \cos\left\{ 2\pi \left[f_j + \left(m - \frac{M-1}{2} \right) R_s \right] t \right\} \right)^2 \quad (18)$$

$$+ \left(\int_{(l-1)T_h+(l-1)T_s}^{(l-1)T_h+lT_s} dt\, r(t) \sqrt{\frac{2}{T_s}} \sin\left\{ 2\pi \left[f_j + \left(m - \frac{M-1}{2} \right) R_s \right] t \right\} \right)^2$$

In conjunction with (15), (17)-(18) define the noncoherent ALR detector for SFH/MFSK signals with discontinuous phase which is shown in Fig. 7.

A comparison of Figs. 5 and 7 serves to illustrate the differences between the optimum noncoherent detectors for FFH/MFSK and SFH/MFSK signals. Both detectors form I & Q components at the symbol level, which undergo identical operations culminating with the zeroth-order Bessel function: this is done for each of the N_c FH channels, however the postprocessing is different. In the FFH case, since there is one symbol per hop, all N_c Bessel outputs are summed for each hop. In the SFH case, the NC channels are partitioned into G = N_c/M M-ary bands corresponding to the G FH carrier frequencies; the Bessel outputs are summed within each M-ary band, and since there are N_s symbols per hop and the carrier phase is assumed to be SI from symbol to symbol, the M-ary outputs are multiplied over all of the symbols in each hop and the resultant is summed over the G carrier frequencies. From a complexity perspective, the only difference is the product over the N_s symbols in each M-ary band on each hop in the SFH case; the single larger summation over the NC channels in Fig. 5 is equivalent to the summations over the M symbols associated with each carrier frequency followed by the summation over the G carrier frequencies.

c. SFH/CPM Signals

Consider SFH signals with arbitrary phase modulation that is continuous over each hop, which is representative of a broad class of signals of interest. The SFH/CPM signal can be written as

$$s(t) = \sqrt{2S} \cos[2\pi f_j t + \phi(\boldsymbol{d}_n, t) - \theta_q]; \quad (l-1)T_h \le t < lT_h \quad (19)$$

where $\phi(\boldsymbol{d}_n, t)$ is the CPM component which depends on the particular M-ary data sequence $\boldsymbol{d}_n$ in the ith hop. The number of distinct data sequences that can occur on a given hop is $N_d = M^s$ and, in the absence of specific channel coding information to the contrary, all sequences' are assumed to be equally likely. For noncoherent detection, the received carrier phase θ_q is modeled as a uniformly distributed RV over (O, 2π) which is assumed to be constant over the entire hop but SI from hop to hop; in the coherent case, we can set . θ_q = O. The separation of the G FH carrier frequencies $\{f_j\}$ is assumed to be uniform and consistent with orthogonality requirements and the contiguous, non-overlapping M-ary band convention of Fig. 4 discussed earlier.

Under these assumptions, the general SFH/CPM signal of (19) can be inserted directly into (16) to determine the ijth likelihood function term. In particular, for coherent detection with θ_q = O,

$$\Lambda_{ij}[r(t)\,|\,f_j] \propto E_{d_n}\left[\exp\left(\frac{2}{N_0}\sqrt{E_h}\int_{(l-1)T_h}^{lT_h} dt\; r(t)\sqrt{\frac{2}{T_h}}\cos[2\pi f_j t+\phi(d_n,t)]\right)\right]$$
$$\propto \sum_{n=1}^{N_d}\exp\left(\frac{2}{N_0}\sqrt{E_h}\int_{(l-1)T_h}^{lT_h} dt\; r(t)\sqrt{\frac{2}{T_h}}\cos[2\pi f_j t+\phi(d_n,t)]\right) \tag{20}$$

which, in conjunction with the universally applicable FH partition expression of (15), defines the optimum coherent detector for *any* SFH/CPM signal.

In the noncoherent case, the likelihood function must also be averaged over the random phase so that

$$\Lambda_{ij}[r(t)\,|\,f_j] \propto \sum_{n=1}^{N_d} I_0\left(\frac{2}{N_0}\sqrt{E_h R_{ijn}}\right) \tag{21}$$

where

$$R_{ijn} \equiv \left(\int_{(l-1)T_h}^{lT_h} dt\; r(t)\sqrt{\frac{2}{T_h}}\cos[2\pi f_j t+\phi(d_n,t)]\right)^2$$
$$+\left(\int_{(l-1)T_h}^{lT_h} dt\; r(t)\sqrt{\frac{2}{T_h}}\sin[2\pi f_j t+\phi(d_n,t)]\right)^2 \tag{22}$$

Combining this result with (15) yields the noncoherent ALR detector, again valid for *any* SFH/CPM signal; the *ij*th representative frequency-time cell is illustrated in Fig. 8. While (21)-(22) is the true theoretical noncoherent *ij*th ALR term, it is not the most practical implementation approach. The relatively complex Bessel operation in (21) results from the expectation over the unknown phase θ_q in each hop. As observed in [25], since the noncoherent ALR involves the joint expectation over this phase and the data sequence in each frequency-time cell, and these operations are linear, the phase expectation can be performed last. In particular, θ_q can be inserted into (20) and the expectation of this expression can be computed over this random phase:

$$Au[r(t)\,|\,f_j] \propto E_{\theta_q}\left[\sum_{n=1}^{N_d}\exp\left(\frac{2}{N_0}\sqrt{E_h}\int_{(l-1)T_h}^{lT_h} dt\; r(t)\sqrt{\frac{2}{T_h}}\cos[2\pi f_j t+\phi(d_n,t)-\theta_q]\right)\right]$$
$$\propto \frac{1}{Q}\sum_{q=1}^{Q}\sum_{n=1}^{N_d}\exp\left(\frac{2}{N_0}\sqrt{E_h}\int_{(l-1)T_h}^{lT_h} dt\; r(t)\sqrt{\frac{2}{T_h}}\cos[2\pi f_j t+\phi(d_n,t)-\theta_q]\right) \tag{23}$$

where the continuous phase expectation has been approximated by an average over Q discrete phases uniformly spaced over the sufficient range $[0, \pi)$.

From a complexity perspective, a tremendous penalty must' be paid to optimally detect an SFH signal with continuous phase over each hop if the coherent or noncoherent ALR is implemented as in (20) or (23) respectively. Since the number of data patterns N_d that must be examined within each M-ary band for each FH carrier frequency on each hop grows exponentially with the number of symbols per hop N_s, the complexity can be impractical even for binary ($M = 2$) data modulation unless N_s is sufficiently small. It is shown later in the SFH/CPFSK case that this increased complexity is counterbalanced by a dramatic improvement in noncoherent ALR detector performance relative to the discontinuous-phase SFH/MFSK case of Fig. 7. It is also shown that for certain modulation indices h, the coherent and noncoherent ALR SFH/CPFSK detectors can be implemented in such a way that the complexity grows linearly rather than exponentially with N_s [25].

D. SFH/CPFSK Signals

For arbitrary modulation index h, the signals of interest are given by (19) with

$$\phi(d_n, t) = 2\pi h R_s \int_{(l-1)T_h}^{t} d\tau \; p(d_n, \tau); \; t \le lT_h \tag{24}$$

where the M-ary data stream is defined by

$$p(d_n, t) = m - \frac{M-1}{2} \; ; \; (l-1)T_h + (l-1)T_s < t < (l-1)T_h + lT_s \tag{25}$$

and $m \in \{0, 1, \ldots, M-1\}$ is the lth data symbol in the ith hop, $l = 1, 2, \ldots N_s$ for the nth data sequence d_n. Equations (24) and (25) define a phase tree for all possible data sequences on the ith hop with arbitrary modulation index and data alphabet size; for example, Fig. 9 illustrates the phase tree for the special case of $M = 4$, $h = \%$. The slope of a particular phase tree branch determines the frequency offset for the corresponding symbol relative to the FH carrier frequency. The frequency transmitted during a given symbol duration is $f_l + [m - lA(M-1)]hR_s$ so that the spacing between adjacent M-ary tones is hR_s. The branches of the phase tree are labelled with the data symbol m and the symbol transitions with the phase state; since $\phi(d_n, t)$ appears in the argument of a sinusoid, these phase states can be reduced to the range $[0, 2\pi)$ by expressing the actual phase modulo 2π as shown in Fig. 9. For the special case of integer sub-multiple modulation indices, i.e., $h = 1/K$ where K is integer, the phase tree alternates between two disjoint sets of K possible states on each successive symbol transition. This reduces the phase tree with M^{N_s} branches for each hop to a trellis with KMN_s branches as shown in Fig. 10 for $M = 4$, $h = \frac{1}{2}$: that is, the data-dependent phase-tree complexity has been changed from an exponential to a linear dependence on N_s.

For the coherent detection case, the minimum CPFSK tone separation for orthogonality is achieved with $h = \frac{1}{2}$, which is usually referred to as minimum shift-keying (MSK). However, for simplicity, first consider the special case $h = 1$, which corresponds to

the minimum separation for *noncoherent* detection. For this particular modulation index the phase state ψ_k at each symbol transition incompletely deterministic independent of the data sequence, alternating between O and π: i.e., at the beginning of the *l*th symbol baud, $\psi_k = (1\text{-}1) \bmod 2\pi$. Then the general SFH/CPM signal of (19) simplifies to the mathematical form of (14) with the addition of ψ_k for the initial phase state of the *l*th symbol (an important difference here is that the received carrier phase θ_q is constant over the entire hop for CPFSK modulation whereas it was only constant over each symbol in the discontinuous-phase MFSK case). In summary, for SFH/CPFSK modulation with $h = 1$, the received signal is independent and identically distributed (i.i.d.) from symbol to symbol conditioned on the FH carrier frequency f_j and the received hop carrier phase θ_q. As is shown later, this is a sufficient condition for drastically simplifying the ALR SFH/CPM detector structure in both the coherent and noncoherent cases.

For coherent detection with $h = 1$ and $\theta_q = 0$, this conditional i.i.d. characteristic allows (20) to simplify as follows:

$$\Lambda_{ij}[r(t) \mid f_j] \propto E_{d_n} \left| \sum_{l=1}^{\cdot} \frac{2}{N_0} \sqrt{E_s} \int_{(l-1)T_h+(l-1)T_s}^{\cdot} dt\, r(t) \sqrt{\frac{2}{T_s}} \cos\left\{ 2\pi \left[f_j + \left(m - \frac{M-1}{2} \right) R_s \right] t + (l-1)\pi \right\} \right| \tag{26}$$

$$\propto \prod_{l=1}^{N_s} \sum_{m=0}^{M-1} \exp\left(\frac{2}{N_0} \sqrt{E_s} \int_{(l-1)T_h+(l-1)T_s}^{(l-1)T_h+lT_s} dt\, r(t) \sqrt{\frac{2}{T_s}} \cos\left\{ 2\pi \left[f_j + \left(m - \frac{M-1}{2} \right) R_s \right] t + (l-1)\pi \right\} \right)$$

This is a very dramatic reduction in operational complexity relative to the general coherent SFH/CPM detector of (20): M^{Ns} exponential functions must still be computed, but instead of M^{Ns} additions, only N_s M-fold sums must be multiplied (i.e., $N_s M$ mathematical operations). So, with the configuration of (26) for coherently detecting SFH/CPFSK signals with $h = 1$, the complexity now grows linearly with N_s.

The same reduction in complexity can be realized in the noncoherent detection case. As a special case of (23),

$$\Lambda_{ij}[r(t) \mid f_j] \propto \sum_{q=1}^{Q} \prod_{l=1}^{N_s} \sum_{m=0}^{M-1} \exp\left(\frac{2}{N_0} \sqrt{E_s} \right. \tag{27}$$

$$\left. \times \int_{(l-1)T_h+(l-1)T_s}^{(l-1)T_h+lT} dt\, r(t) \sqrt{\frac{2}{T_s}} \cos\left\{ 2\pi \left[f_j + \left(m - \frac{M-1}{2} \right) R_s \right] t + (l-1)\pi - \theta_q \right\} \right|$$

It was found in [25] that sufficient accuracy could be achieved with $Q \sim 16$. This structure for the *ij*th frequency-time cell of the optimum noncoherent SFH/CPFSK detector is illustrated in Fig. 11. As noted in [25] and confirmed by comparing Figs. 7 and 11, the computational

complexity of this essentially optimum detector for continuous-phase MFSK modulation is on the order of that of the optimum detector for the discontinuous-phase case.

Earlier, it was implied that the conditional i.i.d. feature of SFH/CPFSK modulation with $h = 1$ is sufficient but not necessary to reduce the complexity of the coherent or noncoherent ALR detectors from an exponential to a linear dependence on N_s; in fact, similar implementation savings can be realized for all integer sub-multiple modulation indices. For example, in the $M = 4$, $h = \frac{1}{2}$ (MSK) case, Fig. 9 shows that the phase state ψ_k alternates between $\{\pi/2, 3\pi/2\}$ and $\{0, \pi\}$ for the beginning of the even and odd symbol bauds respectively. However, instead of a fully-connected trellis with alternating pairs of states, it may be more convenient to consider a 4-state trellis which is semi-connected as shown in Fig. 10.

Consider the general case of coherent detection of CPFSK signals with $h = 1/K$ and arbitrary M. Analogous to Fig. 10, the CPFSK phase trellis is semi-connected with $2K$ states at each symbol transition, Let d_l denote a particular data sequence over the first l symbols of the ith hop, and let $D_{l,k}$ denote the set of all such data sequences that end at the kth phase state, ψ_k. As a variation on (20), define the conditional partial metric

$$\Delta_{l,k} \equiv \sum_{d_l \in D_{l,k}} \exp\left(\frac{2}{N_0}\sqrt{E_s}\int_{(l-1)T_h}^{(l-1)T_h+lT_s} dt\, r(t)\sqrt{\frac{2}{T_s}}\cos[2\pi f_j t + \phi(d_l, t)]\right) \quad (28)$$

where the average in (28) is only over those l-symbol sequences d_l that lie in $D_{l,k}$. Note that

$$\Lambda_{ij}[\, r(t) \mid f_j, d_{N_s} \in D_{N_s,k}] \propto \Delta_{N_s,k} \quad (29)$$

so that

$$\Lambda_{ij}[r(t) \mid f_j] \propto \sum_{k=1}^{2K} \Delta_{N_s,k} \quad (30)$$

The conditional partial metric $A_{l,k}$ should not be interpreted as a conditional partial ALR, nor should (28) be used to compute it since the number of data sequences in $D_{l,k}$ grows exponentially with the sequence length l. In fact, the phase trellis can be used to establish a recursive expression for the lth conditional partial metric $A_{l,k}$ in terms of the $(l-1)$th metrics. Let $M_{k',k}$ be the set of all data symbols m in the trellis diagram that connect the k'th state at the beginning of the lth symbol baud to the kth state at the end. Then (28) yields the recursive relationship

$$\Delta_{l,k} \propto \sum_{k'=1}^{2K} \Delta_{l-1,k'} \sum_{m \in M_{k',k}} \exp\left(\frac{2}{N_0}\sqrt{E_s} \right.$$

$$\left. \times \int_{(l-1)T_h+(l-1)T_s}^{(l-1)T_h+lT} dt\, r(t) \sqrt{\frac{2}{T_s}} \cos\left\{ 2\pi \left[f_j + \left(m - \frac{M-1}{2} \right) R_s \right] t + \psi_{k'} \right\} \right| \tag{31}$$

and, for the initial symbol baud $l = 1$,

$$A_{1,k} \propto \sum_{m \in M_{k',k}} \exp\left(\frac{2}{N_0}\sqrt{E_s} \int_{(l-1)T_h}^{(l-1)T_h+T_s} dt\, r(t) \right. \Gamma + {}^{ws}[^{2}\,,,[\,,^{+}(^{m}\text{-wi}^{t}\}) \left. \right) \,,32)$$

where k' is the particular state for which the phase $\psi_{k'} = O$. Equations (31)-(32) can now be applied to compute $\Delta_{l,k}$ for $l = 2, 3, \ldots, N_s$, and then (30) can be used to calculate the ijth ALR function.

Of course, for SFH/CPM signals where $1/h$ is not an integer, this trellis structure is not applicable. This is unfortunately the case for some currently deployed tactical SHF transceivers such as the U.S. Army's Single-Channel Ground and Airborne Radio System (SINCGARS) and the British Jam-Guarded Radio (JAGUAR), which employ duobinary FM rather than CPFSK modulation, but with $h = 0.7$ [28], [29]. in principle, the general coherent and noncoherent SFH/CPM detectors of (20) and (21)-(22) (or Fig. 8) are still available. However, SINCGARS and JAGUAR have a maximum data symbol rate $R_s = 16$ ksymbols/sec with a nominal hop rate R_h - 100 hops/see, so that each hop contains approximately $N_s = R_s/R_h \sim$ 160 symbols. So we would need to consider $N_d \sim 2^{160}$ distinct data patterns for each frequency-time cell, Furthermore, these radios cover the VHF range 30-88 MHz (i.e., W_{ss} = 58 MHz) with 25 kHz channels so that there are G = 2320 FH carrier frequencies. Therefore, the computational complexity of the generai SFH/CPM detector structure makes this implementation impractical.

IV. Suboptimum SFH Detectors

A. FBC and WE

For comparison with the performance of the optimum noncoherent detectors derived above, the traditional noncoherent FFH FBC and the WE detector are extended to the SFH/MFSK case with minimum tone separation R_s for orthogonality ($h = 1$ again) and non-overlapping M-ary bands.

As shown in Fig. 12 for the FBC, for each data symbol on each hop within each M-ary band, the received signal is fed to a simple noncoherent, unmodulated-carrier, i & Q demodulator, and these outputs are then squared and summed. Within each frequency-time cell, these SI χ^2 RVS with 2 degrees of freedom are summed over the N_s data symbols in

each hop creating a X^2RV R_{ij} with $2N_s$ degrees of freedom; these are compared with a threshold η which is the same for all such cells. If this threshold is exceeded for any of the G bands on a given hop, the OR gate generates a"1"; otherwise, it outputs a "O". These numbers are then summed over all N_h observed hops and compared with a second integer threshold L. The two thresholds are jointly optimized to minimize P_M for the selected P_{FA} and received SNR. Although this structure is suboptimum, it shall be shown that it performs almost as well as the ALR noncoherent detector for SFH/MFSK signals with discontinuous phase.

In the WE case, the metric of (6) is used with $W_m = MR_s$, N_c replaced by G, and the radiometer-derived R_{ij}s replaced by the I & Q generated R_{ij}s of Fig. 12 calculated for each of the $G = N_c/M$ bands. Since the WE detector is optimum conditioned on this channelized preprocessor, it can be expected to outperform the FBC.

B. Maximum-Likelihood Ratio FH Detectors

In deriving the ALR detectors for the various SFH signals considered, it was assumed that the data sequences within each hop and the FH pattern were unknown and equally likely. Furthermore, in the noncoherent case, the received carrier phase was assumed to be unknown and uniformly distributed over [0, 2π). Consequently, the optimum detectors had to average over each of these signal characteristics. An alternative approach is to jointly detect the presence of the signal while simultaneously estimating one or more of these unknown signal attributes (sometimes referred to as "feature extraction") under H_1 using an MLR signal processor.[6] By definition, an ALR receiver must perform better from a pure detection perspective than any MLR structure; however, in many cases the detection performance is almost the same, the MLR format may be easier to analyze or less complex to implement, and the derived signal feature is of interest.

For example, consider the previously derived ALR coherent and noncoherent detectors for SFH/CPFSK signals with $h = 1$. The summation (average) over the Q discrete phases in the noncoherent detector of Fig. 11 could be replaced by a maximization function to jointly detect the signal and determine the (discretized) received carrier phase. Mathematically, this MLR detector would replace (27) by the ijth likelihood function

$$\Lambda_{ij}[r(t) \mid f_j] \propto \max_{q=1}^{Q} \left[\prod_{l=1}^{N_s} \sum_{m=0}^{M-1} \exp\left(\frac{2}{N_0} \sqrt{E_s} \right. \right. \times \left. \left. \int_{(l-1)T_h+(l-1)T_s}^{(l-1)T_h+lT_s} dt\, r(t) \sqrt{\frac{2}{T_s}} \cos\left\{ 2\pi \left[f_j + \left(m - \frac{M-1}{2} \right) R_s \right] t + (l-1)\pi - \theta_q \right\} \right) \right] \tag{33}$$

To simultaneously detect the signal and determine the FH pattern, (15) is replaced by

[6] Van Trees calls these metrics generalized likelihood ratios [1, p. 92].

$$\Lambda[r(t)] \propto \prod_{l=1}^{N_h} \max_{j=1}^{G} \{\Lambda_{lj}[r(t) \mid f_j]\} \tag{34}$$

where Λ_{lj} is given by (26) or (27) for the coherent or noncoherent cases respectively. Finally, for joint signal and data detection (sometimes referred to as a "copy" function), the summation over the M data symbols in (26) or (27) is replaced by a maximization. In particular, for coherently detecting the signal while estimating the imbedded data sequence, use the ijth likelihood function

$$\Lambda_{lj}[r(t) \mid f_j] \propto \prod_{l=1}^{N_s} \max_{m=0}^{M-1} \left[\exp\left(\frac{2}{N_0}\sqrt{E_s} \right. \right.$$

$$\left. \left. \times \int_{(l-1)T_h+(l-1)T_s}^{(l-1)T_h+lT_s} dt\, r(t) \sqrt{\frac{2}{T_s}} \cos\left\{ 2\pi \left[f_j + \left(m - \frac{M-1}{2} \right) R_s \right] t + (l-1)\pi \right\} \right) \right] \tag{35}$$

V. Performance Example for Various SFH/BFSK Detectors

To appreciate the relative performance of the derived optimum and suboptimum SFH/MFSK detectors, consider the following example. As was done throughout this paper, assume an idealized situation in which the detector has acquired perfect side information about all of the usual received signal parameters including hop timing epoch. Of course, it is not assumed that the detector has *a priori* knowledge about the particular FH pattern or data sequence. For the ALR and MLR receivers, unless stated otherwise, CPFSK data modulation is assumed to demonstrate the extent to which the continuous-phase characteristic can be exploited by a properly designed detector.

For ease of computational complexity, consider only the case of binary (BFSK) data modulation. Using the previously defined notation, the received SFH/BFSK signal is assumed to have the following parameters:

W_{ss} = 10 MHz $\qquad$ R_h = 100 hops/see

T = 0.2 sec $\qquad$ R_s = *10* Ksymbols/sec

1

$G = W_{ss}/R_s$ = *1000* binary bands: coherent detection (i.e., h = ½)

G = $W_{ss}/2R_s$ = 500 binary bands; noncoherent detection (i.e., h = 1)

$N_h = R_h T$ = *20* consecutive hops

$N_s = R_s/R_h$ = *100* symbols/hop

The performance of various SFH/BFSK detectors discussed in this paper was plotted for these signal characteristics in Fig. 13 as P_M versus the received signal-to-noise ratio $\gamma = S/N_0W_{ss}$ for fixed $P_{FA} = 10^{-3}$ based on a combination of analytical and computer simulation techniques. These detectors include the wideband radiometer, WE, FBC, noncoherent ALR discontinuous- and continuous-phase, and coherent ALR and MLR discontinuous-phase structures, where the MLR receiver jointly detects the signal and estimates the data.

There is always a strong motivation to simplify the performance computation task by liberally applying CLT arguments to approximate sums of large numbers of i.i.d. RVS by a single GRV. However, as was noted earlier in conjunction with the WE detector, it is well known that when the PDFs of the i.i.d. RVS have long tails, the convergence of their sum to a GRV is very slow rendering the CLT approximation inaccurate and often leading to overly optimistic performance results. For this reason, the performance of most of the detectors in Fig. 13 was based on novel computer simulation techniques described in depth in [24] and [25] and which will not be repeated here.

Looking at the curves in Fig. 13, the radiometer performance was simply based on the closed-form approximation of (4), for which the CLT approach is accurate. As a performance benchmark, it achieves $PM = 10^{-2}$ (for $P_{FA} = 10^{-3}$) at y = -24.2 dB.

The FBC curve was determined for the structure of Fig. 12 using a purely analytical approach. In the ijth frequency-time cell, R_{ij} is a central (for the G-1 noise-only bands under H_1 or all G bands under H_0) or non-central (for the remaining signal-plus-noise band under H_1) χ^2 RV with $2N_s = 200$ degrees of freedom. The probability that each of these SI RVS exceeds the common threshold η can be readily calculated; then the probability that the OR gate generates a "O" or a "l" on a given hop can be computed. The final summation over the $N_h = 20$ observed hops is then a well-defined binomial RV, and the probability that it exceeds the second integer threshold L (jointly optimized with η) can be calculated as in *[15,* Vol. Ill, pp. 295-300]. Actually, for the parameters in this example, $L = 5$ was optimum over most of the range in Fig. 13. In particular, the FBC required y = – 32.4 dB at the benchmark value of *PM* which is almost 8 dB better than the radiometer performance. As noted earlier, although it is suboptimum, the FBC performs as well as it does because it is channelized to match the hypothesized received FH signal.

The WE performance in Fig. 13 was based on the approach discussed in Section IV.A. using computer simulation techniques described in [25]. Surprisingly, its performance is only negligibly inferior to the noncoherent ALR discontinuous-phase detector over the entire range in Fig. 13.

The noncoherent ALR SFH/BFSK performance curve was based on the detector of Fig. 7 using computer simulation techniques described in [25]. It is moderately better than the FBC performance: in particular, at $PM = 10^{-2}$, it requires y = *-33.0* dB, which is only 0.7 dB better than the FBC.

Just as the channelized detectors performed significantly better than the wideband energy detector, Fig. 13 shows that the continuous-phase characteristic results in another major performance improvement for ALR noncoherent detectors. The computer-simulated performance curve for the latter case is based on the structure of Fig. 8 with $Q = 16$ discrete phases uniformly spaced over $[0, \pi)$. It requires $\gamma = -38.7$ dB at $P_M = 10^{-2}$, which is remarkably almost 6 dB better than the discontinuous-phase BFSK case. This is an indication of the degree to which optimum noncoherent detectors can exploit CPM signaling.

Finally we come to the coherent ALR and MLR detectors for SFH/BFSK signals with $h = \frac{1}{2}$. The tones are now spaced $R_s/2$ apart and there are G = 1000 M-ary bands. The performance for the discontinuous-phase case was actually simulated, but, because coherent detection is assumed, it is assumed that the received phase for each symbol is known. That is, the received signal is given by (14) with $M = 2$, R_s replaced by $R_s/2$, and $\theta_0 = 0$, and the ijth likelihood function for the ALR and MLR[7] detectors are given by (25) and (29) respectively, again with $M = 2$ and R_s replaced by $R_s/2$. It must be stressed that this assumption of symbol-by-symbol phase coherence in the receiver is not meant to be a realizable condition: rather it is intended as a vehicle for comparison with the ALR noncoherent detector performance. From this perspective, it is evident that *both coherent defectors are only marginally better than the noncoherent ALR CPFSK detector.* In particular, at $P_M = 10^{-2}$ the coherent MLR and ALR detectors perform 0.2 dB and 0.6 dB better respectively than the ALR noncoherent detector.

Note that the performance curves in Fig. 13 are grouped into three quality levels. (1) The worst is the radiometer which is noncoherent and unchannelized. (2) The intermediate detectors, which include the FBC, WE and noncoherent ALR for discontinuous phase and perform about 9 dB better than the radiometer, are all channelized to match the FH frequencies but are noncoherent and not designed to exploit continuous-phase signals. (3) Finally, the noncoherent ALR continuous-phase and coherent ALR and MLR detectors perform about 15 dB better than the radiometer.

It is worthwhile mentioning that all of the computer simulated curves in Fig. 13 were CPU-intensive. Each typically is based on a spline curvefit through 5-6 performance simulation points, with each point representing about 40,000 trials requiring approximately 2 days to generate on a SPARCstation using the techniques described in [24] and [25].

VI. Conclusions

This paper presented a comprehensive analysis of optimum and previously published suboptimum detectors for FH signals intercepted in AWGN. All of the SFH detector structures derived herein represent new contributions in this area. Particular attention was given to SFH/CPM signals. Implementable optimum detection algorithms were derived for the special case of SFH/CPFSK signals with integer sub-multiple modulation indices. Novel techniques for accurate computer simulation of the performance of these detectors were used to compare their relative capabilities, A fundamental observation is that CPM signals can be exploited by sophisticated albeit practical noncoherent detectors, with performance comparable to the best coherent detection schemes.

---

[7]Although, as discussed in Section IV.B, there are several possible MLR structures, this example refers to joint coherent detection of the SFH/BFSK signal and the imbedded data.

REFERENCES

[1] H. L. Van Trees, *Detection, Estimation, and Modulation Theory, Part I*, John Wiley, New York, NY, 1968.

[2] L. E. Brennan, 1. S. Reed and W. Sollfrey, "A comparison of average-likelihood ratio tests for detecting radar targets of unknown Doppler frequency," *IEEE Transactions on Information Theory,* Vol. IT-14, pp. 104-110, January 1968.

[3] J. V. DiFranco and W. L. Rubin, *Radar Detection,* Prentice-Hall, Englewood Cliffs, NJ, 1968.

[4] J. 1. Marcum, "A statistical theory of target detection by pulsed radar," RAND, Report RM-754, 1947; see also *IRE Transactions on Information Theory,* Vol. IT-6, pp. *59-267,* April *1960.*

[5] W. W. Peterson, T. G. Birdsall and W. C. Fox, "The theory of signal detectability," *IRE Transactions on Information* Theory, Vol. IT-4, pp. 171-212, 1954

[6] 1. Selin, "Detection of coherent radar returns of unknown Doppler shift," *IEEE Transactions on Information Theory,* Vol. IT-11, pp. 396-400, July 1965.

[7] S. M. Kay, "Robust detection by autoregressive spectrum analysis," *IEEE Transactions on Acoustics, Speech, and Signal Processing,* Vol. ASSP-30, No. 2, pp. 256-269, April 1982.

[8] H. Urkowitz, "Energy detection of unknown deterministic signals," *Proceedings of the IEEE*, Vol. 55, No, 4, pp. 523-531, April 1967.

[9] J. D. Bruce and K. D. Snow, "Final technical report Teal Wing program," Probe Systems, Report PSI-ER 327, October 1974.

[10] J. D. Eden, "Wideband, noncoherent, frequency-hopped waveforms and their hybrids in low-probability-of-interecept communications," U. S. Naval Research Laboratory, Report No. 8025, November 1976.

[11] D. G. Woodring and J. D. Eden, "Detectability calculation techniques," U. S. Naval Research Laboratory, Report No. 1977-1, September, 1977.

[12] D. G. Woodring, "Performance of optimum and suboptimum detectors for spread spectrum waveforms," U. S. Naval Research Laboratory, Report No. 8432, December 1980.

[13] R. A. Dillard, "Detectability of spread-spectrum signals," *IEEE Transactions on Aerospace and Electronic Systems,* Vol. AES-15, No. 4, pp. 526-537, July 1979.

[14] R. A. Dillard and G. A. Dillard, *Detectability of Spread Spectrum Signals,* Artech House, Norwood, MA, 1989.

[15] M. K. Simon, J. K. Omura, R. A. Scholtz and B. K. Levitt, *Spread Spectrum Communications,* Computer Science Press, Rockville, MD, 1985.

[16] D. J. Torrieri, *Principles of Secure Communication Systems,* Artech House, Norwood, MA, 1985.

[17] D. L. Nicholson, *Spread Spectrum Signal Design,* Computer Science Press, Rockville, MD, 1985.

[18] N. C. Beaulieu, W. L. Hopkins and P. J. McLane, "Interception of frequency-hopped spread-spectrum signals," *IEEE Journal on Selected Areas of Communications,* Vol. 8, No. 5, pp. 854-855, June 1990.

[19] A. Polydoros and K. T. Woo, "LPI detection of frequency-hopping signals using autocorrelation techniques," *IEEE Journal on Selected Areas in Communications,* Vol. SAC-3, No. 5, pp. 714-726, September 1985.

[20] A. Polydoros and C. L. Nikias, "Detection of unknown-frequency sinusoids in noise: spectral versus correlation domain," *IEEE Transactions on Acoustics, Speech, and Signal Processing,* Vol. ASSP-35, No. 6, pp. 897-900, June 1987.

[21] W. E. Snelling and E, Geraniotis, "Sequential detection of unknown frequency hopping wave forms," *IEEE Journal on Selected Areas in Communications,* Vol. SAC-7, pp. 602-617, May 1989.

[22] C. D. Chung, "Generalized likelihood-ratio detection of multiple-hop frequency-hopping signals," *MILCOM 91 Conference Record,* pp. 24.1.1-4, Washington, DC, October 1991.

[23] C. D. Chung and A. Polydoros, "Detection and hop-rate estimation of random FH signals via autocorrelation techniques," *MILCOM 91 Conference* Record, pp. 16.1,1-5, Washington, DC, October 1991.

[24] U. Cheng and M. K. Simon, "Statistical models for evaluating the performance of coherent slow frequency-hopped M-FSK intercept receivers," submitted for publication to *IEEE Transactions on Communications.*

[25] U. Cheng, M. K. Simon, B. K. Levitt, and A. Polydoros, "Statistical models for evaluating the performance of noncoherent slow frequency-hopped M-FSK intercept receivers," submitted for publication to *IEEE* Transactions on Communications.

[26] D. J. Torrieri, *Principles of Military Communication Systems,* Artech House, Dedham, MA, 1981.

[27] W. E. Snelling, "New methods for the detection and interception of frequency-hopped waveforms," Johns Hopkins University Applied Physics Laboratory, Technical Memorandum JHU/APL TG 1378, p. 15, November 1990.

[28] T. T. Tjhung and P. H. Wittke, "Carrier Transmission of Binary Data in a Restricted Band," *IEEE Transactions on Communication Technology,* Vol. COM-18, *No. 4,* pp. 295-304, August 1970.

[29] T. T. Tjhung, C. S. Ng, K. K. Yeo and P. H. Wittke, "Error performance analysis for narrow-band duobinary FM with discriminator detection," *IEEE Transactions on Communications,* Vol. COM-33, No. *5,* pp. 399-408, May 1985.

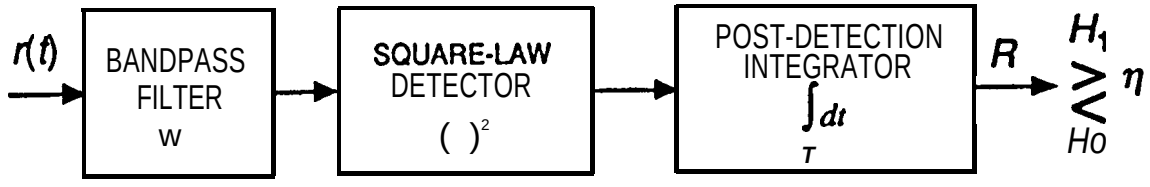

Fig. 1. Wideband energy detector or radiometer.

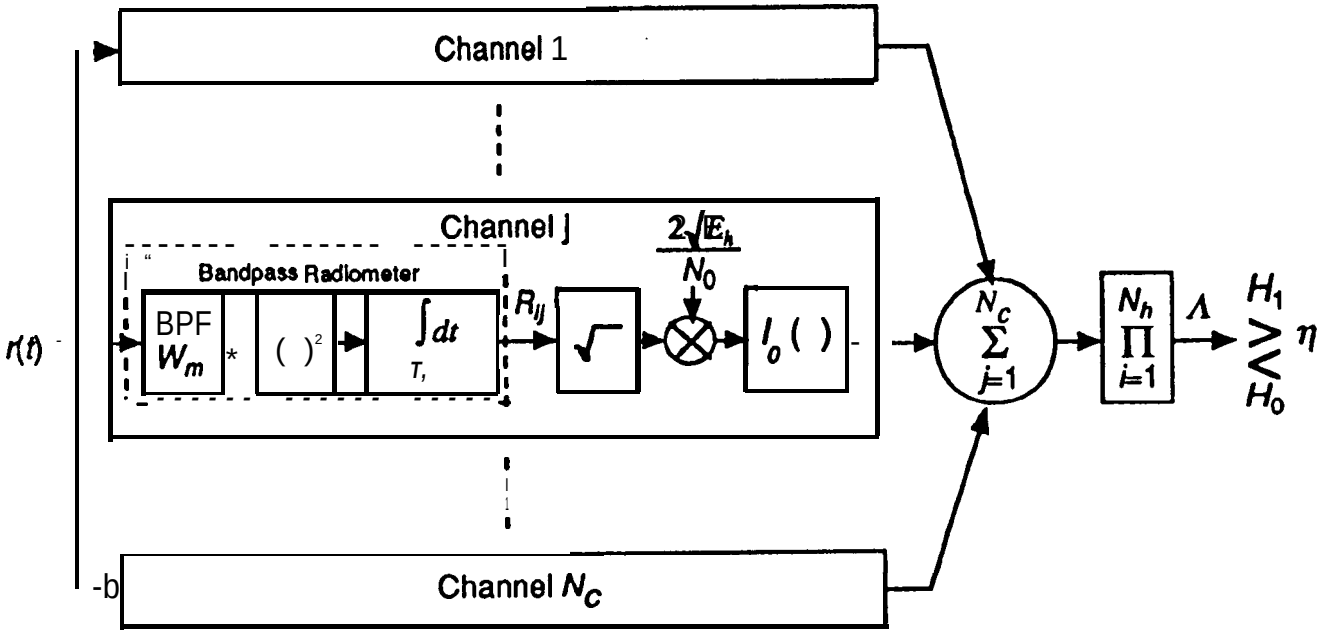

Fig. *2.* Woodring-Edell channelized FH detector for unity time-bandwidth product.

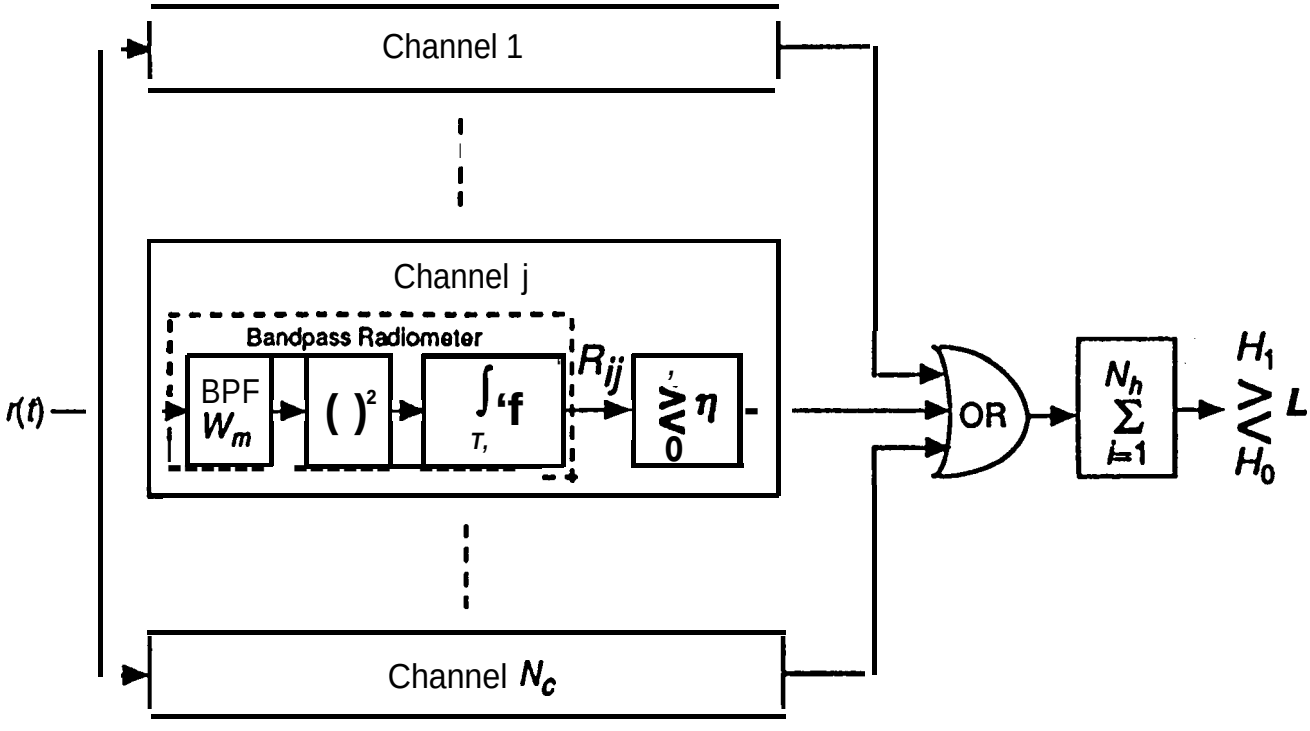

Fig. 3. Bandpass radiometer channelized filter-bank combiner.

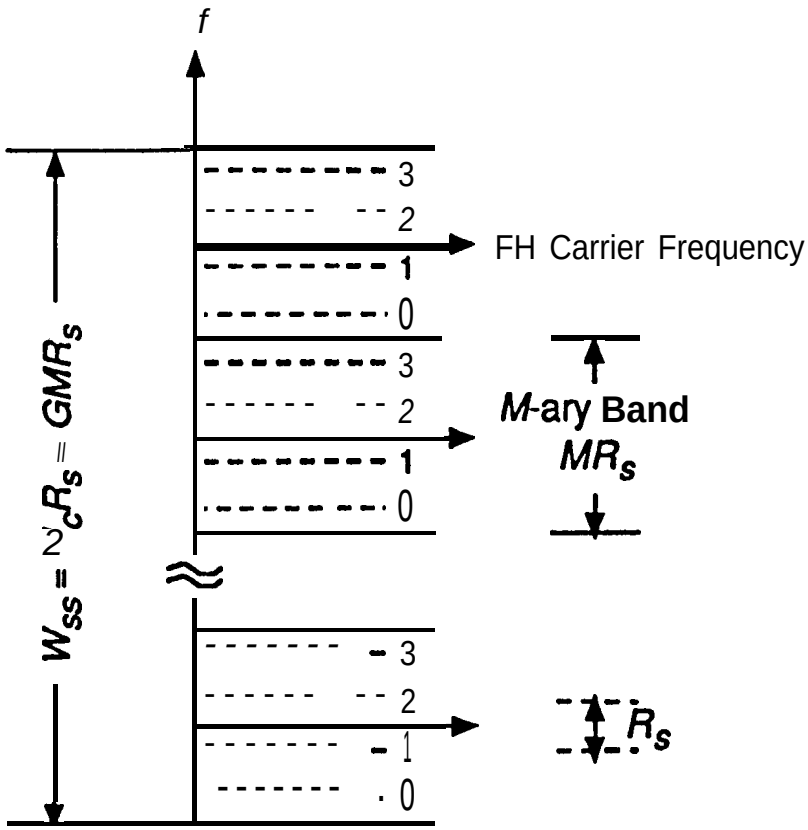

Fig. 4. Non-overlapping *M*-ary band convention.

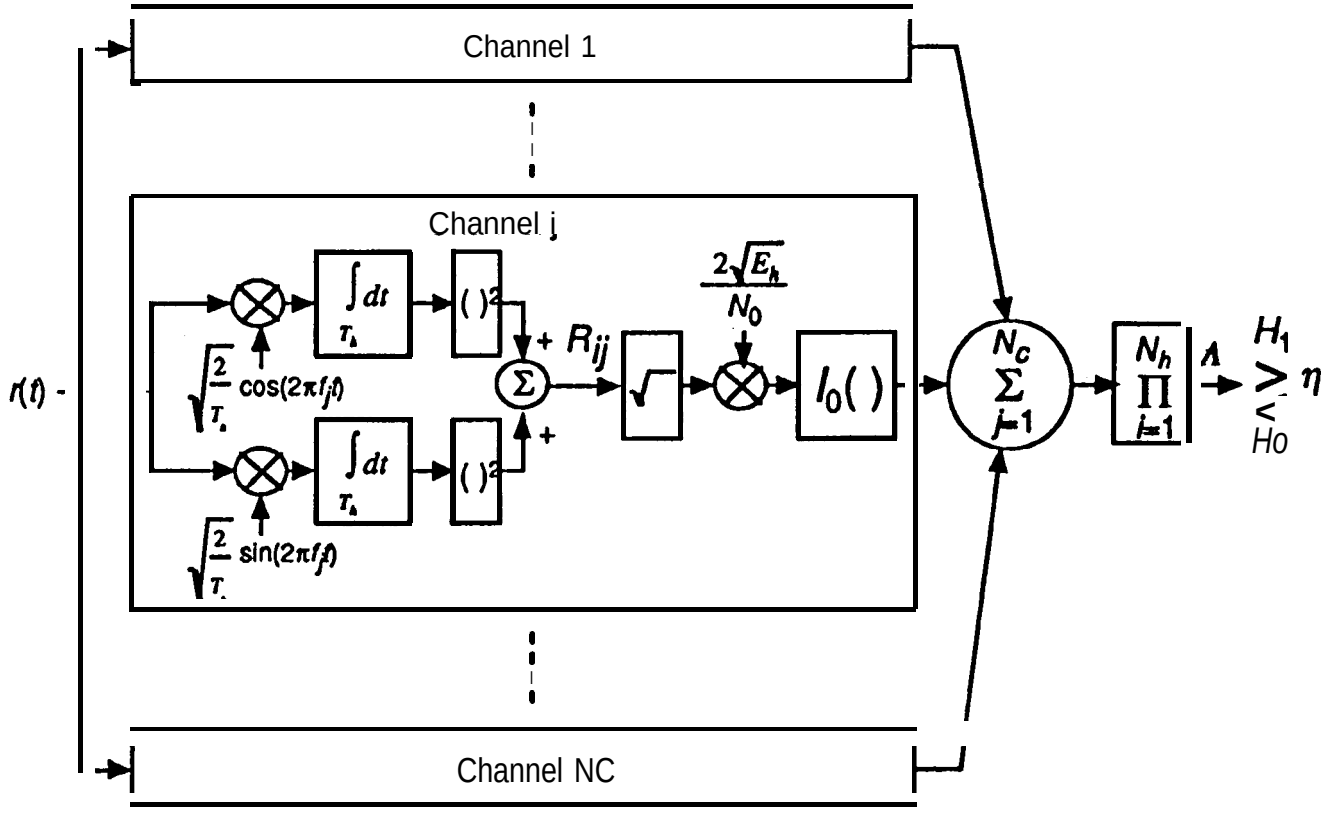

Fig. 5. Noncoherent ALR detector for FFH/MFSK signals.

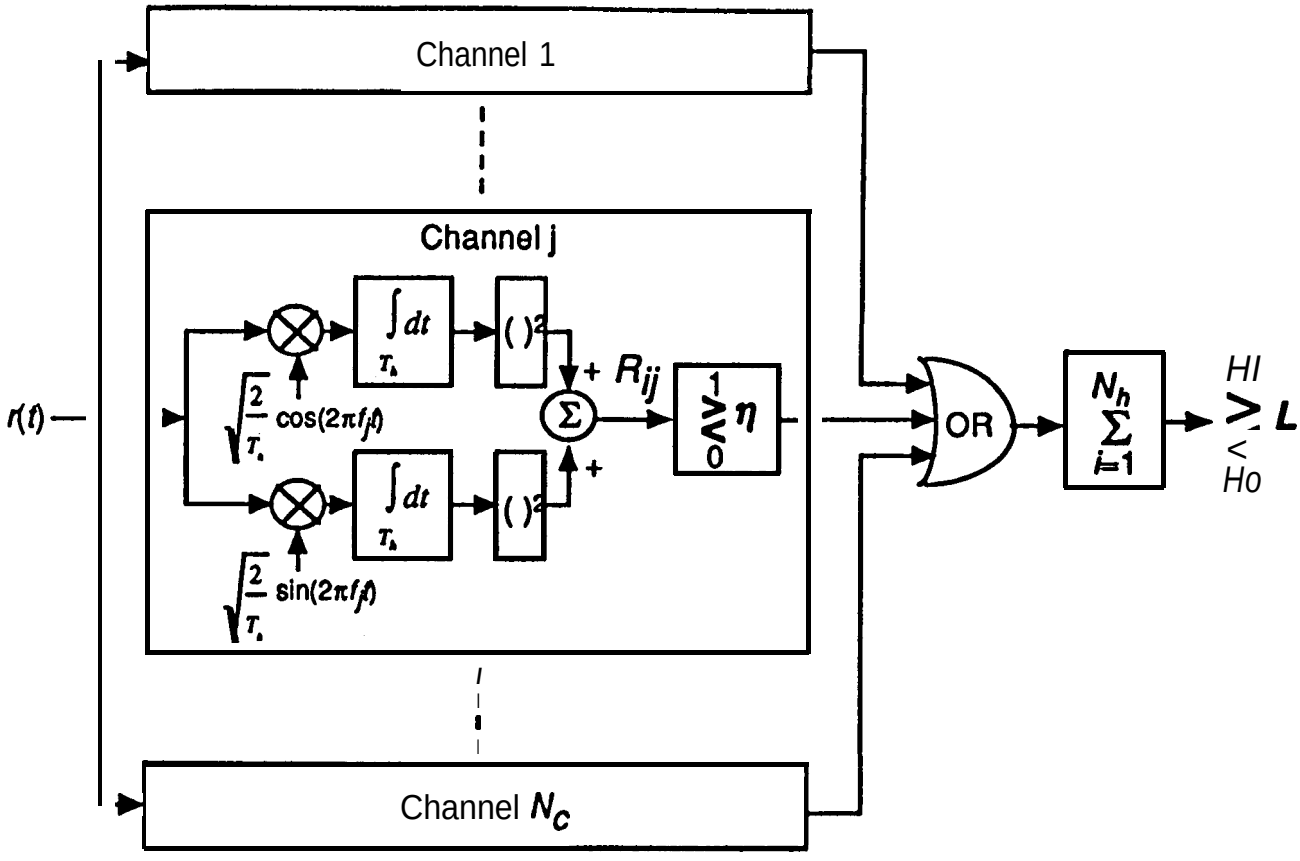

Fig. 6. Noncoherent filter-bank combiner for FFH/MFSK signals.

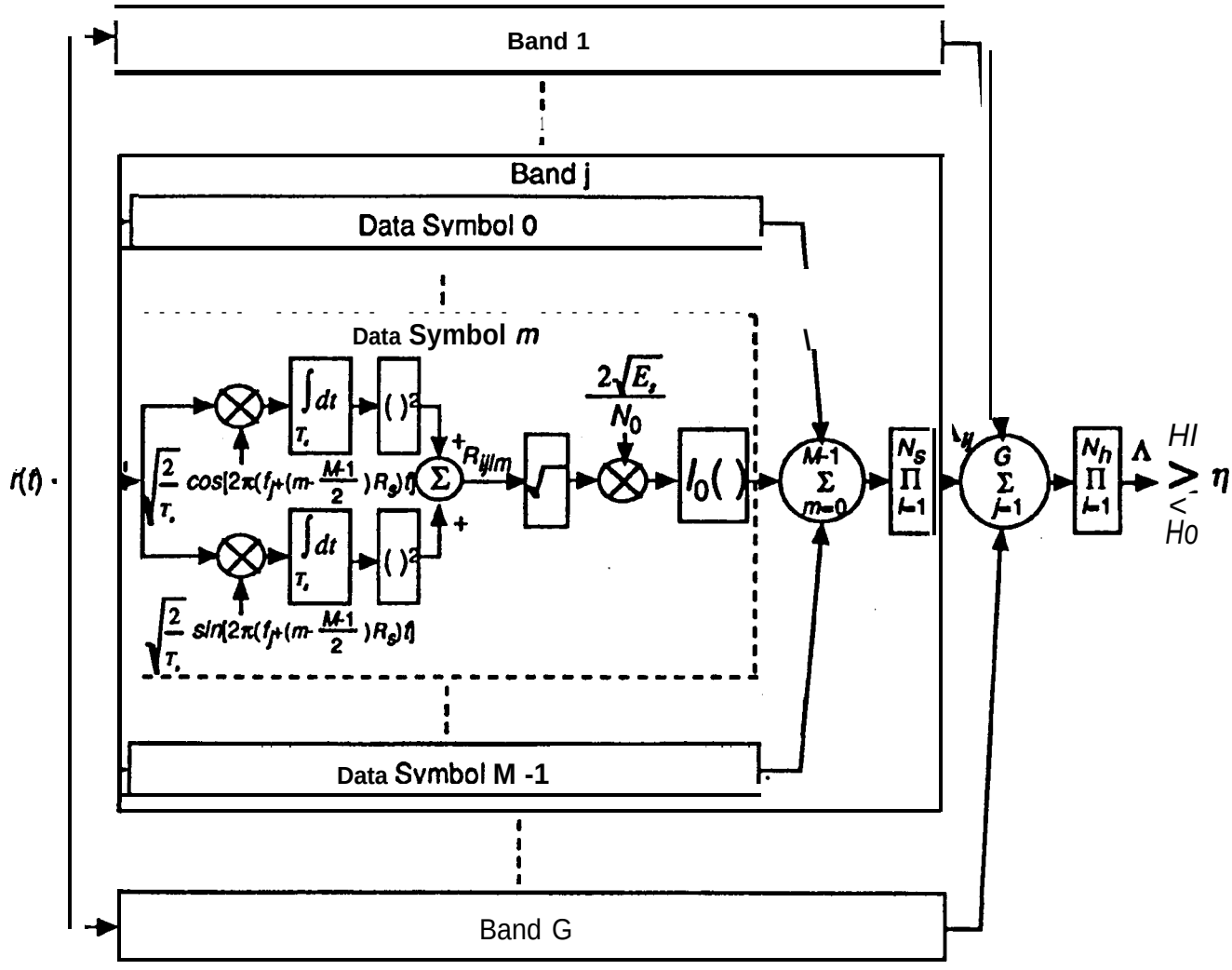

Fig. 7. Noncoherent ALR SFH/MFSK detector when received carrier phase is constant over each symbol but discontinuous (i.e., Sl) from symbol to symbol.

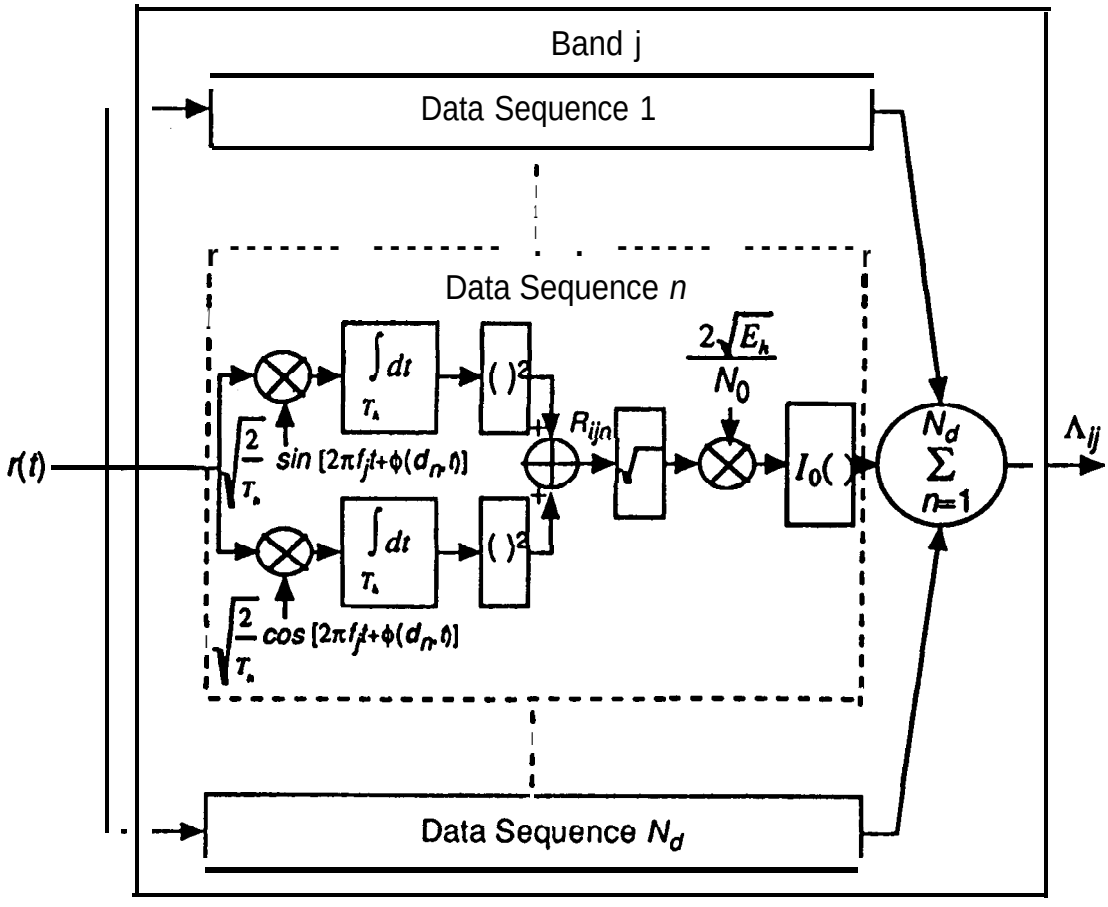

Fig. 8. Representative frequency-time cell for *i*th hop and *j*th *M*-ary band of noncoherent ALR detector for arbitrary SFH/CPM signals.

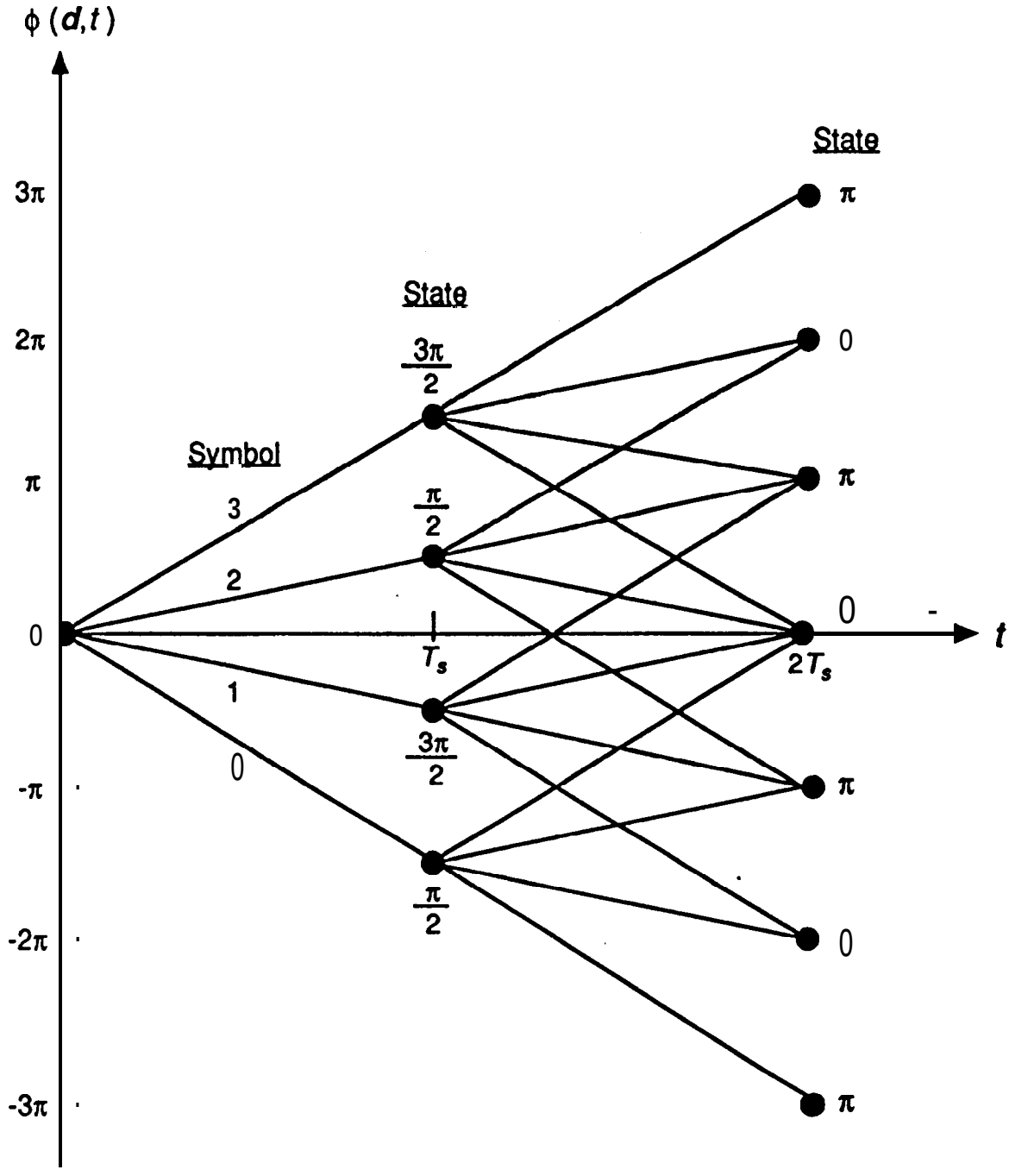

Fig. 9. CPFSK phase tree for the special case $M = 4$, $h = \frac{1}{2}$.

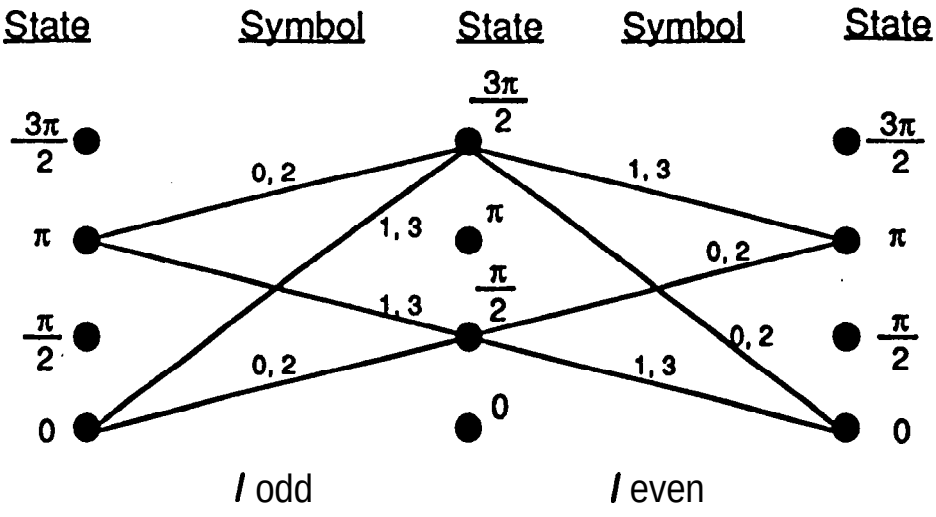

Fig. 10. CPFSK phase trellis for *l*th symbol bauds when $M = 4$, $h = \%$.

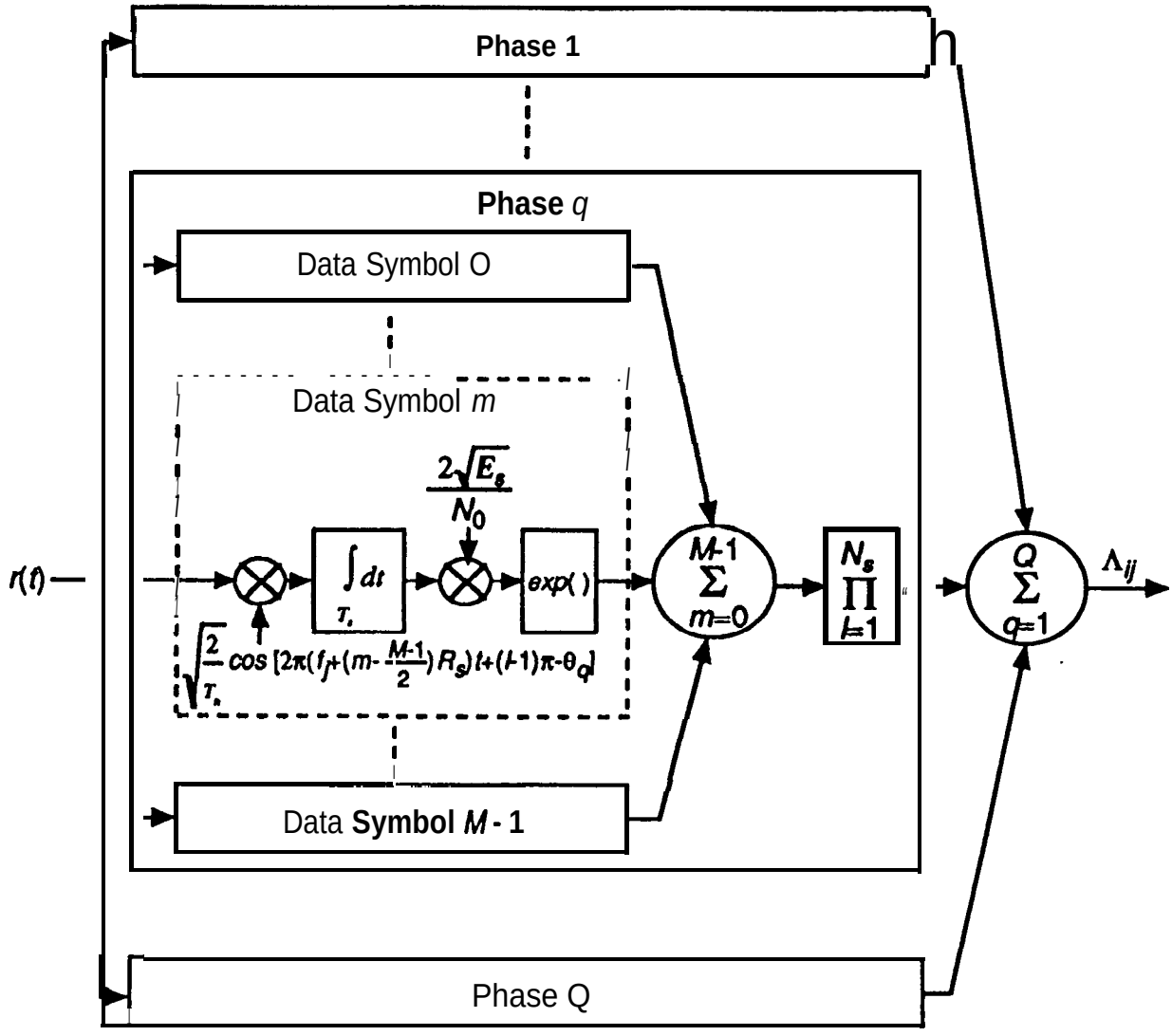

Fig. 11. Representive frequency-time cell of efficient implementation of noncoherent ALR detector for SFH/CPFSK signals with $h = 1$.

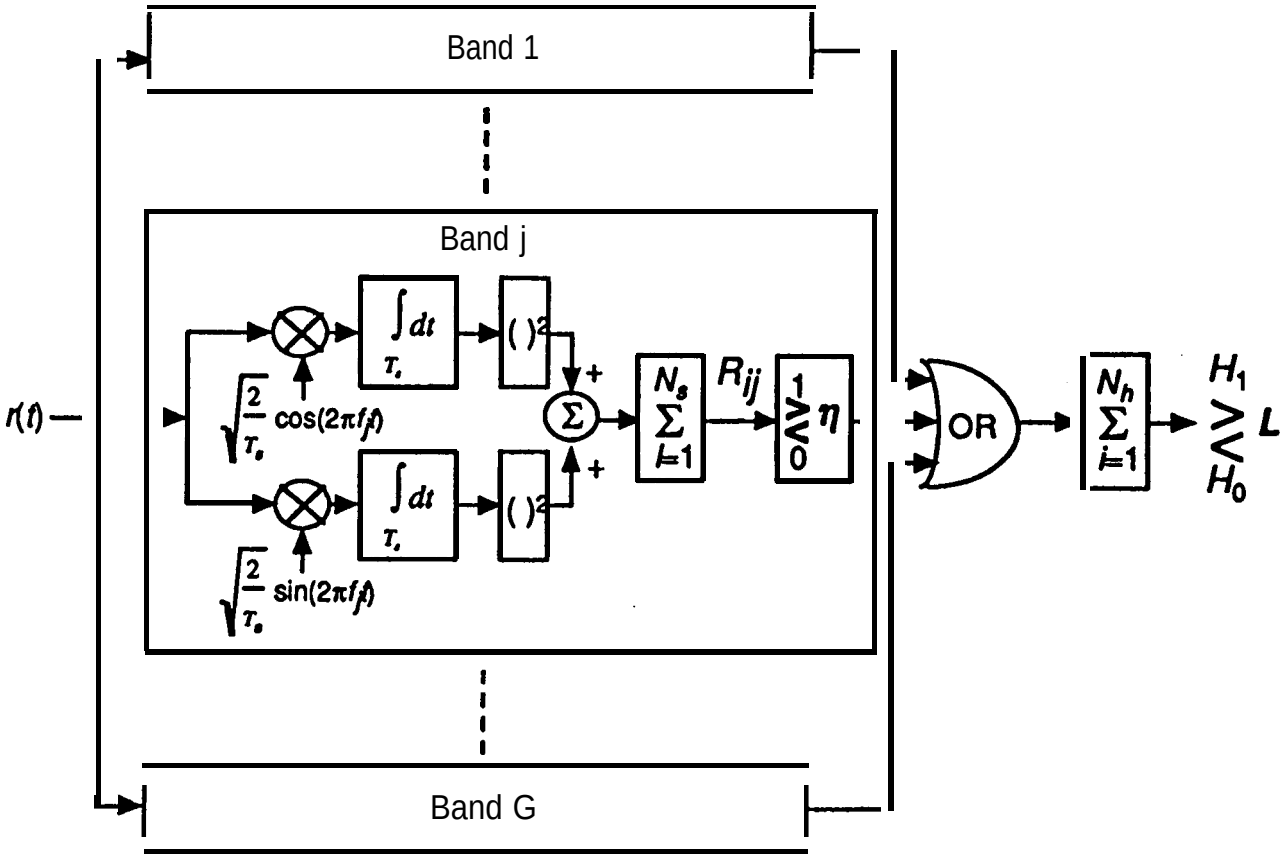

Fig. 12. Filter bank combiner for SFH/MFSK signals.

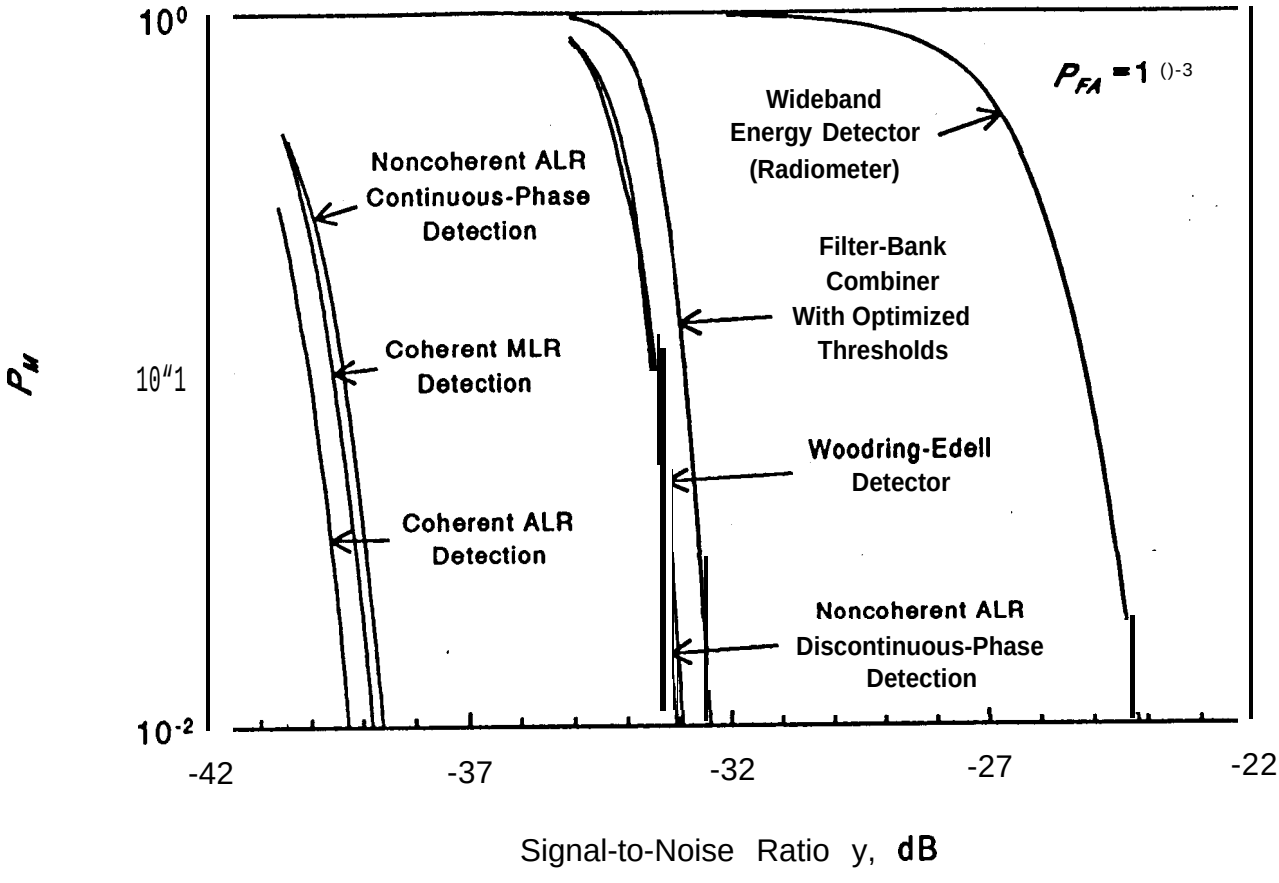

Fig. 13. Performance of SFH/BFSK detectors.